

Supporting Information

Construction of TiO₂/Ti-MOF/MXene Ternary Heterojunction for Enhanced Photocatalytic Nitrogen Fixation

Tianyu Huang, Yangyang Sun*, Houqiang Ji, Jiahui Huang, Wanchang Feng, Zheng Liu, Wenlin Xu, Huan Pang*

School of Chemistry and Materials, Yangzhou University, Yangzhou, Jiangsu 225002,
P. R. China

E-mail: yangyangsun@yzu.edu.cn; panghuan@yzu.edu.cn

1. Experimental reagents

Titanium aluminum carbide (Ti_3AlC_2) is provided by Laizhou Kaikai Ceramic Materials Co., LTD. Tetrabutyltitanate (TBOT), *N,N*-dimethylformamide (DMF) and methanol (CH_3OH) were supplied by Sinophosphoric Chemical Reagents Co., LTD. Terephthalic acid (H_2BDC) is supplied by Shanghai Aladdin Chemical Reagent Co., LTD. Hydrofluoric acid (HF) and hydrochloric acid (HCl) are supplied by Shanghai Sinopod Chemical Reagent Co., LTD., China. Lithium chloride (LiCl) is supplied by Aladdin Reagent. All chemical reagents are used directly without further purification.

1.1 Synthesis of $\text{Ti}_3\text{C}_2\text{T}_x$ MXene

$\text{Ti}_3\text{C}_2\text{T}_x$ MXene nanosheets were synthesized via a combined method of chemical etching and ultrasonic exfoliation. Initially, 1 g of $\text{Ti}_3\text{C}_2\text{T}_x$ (MAX) was added to an etching solution composed of 3 mL deionized water, 6 mL concentrated hydrochloric acid, and 1 mL hydrofluoric acid. The mixture was stirred at 41 °C for 15 hours to selectively remove the Al layers. After the etching process, the resulting suspension was centrifuged at 4500 rpm and washed repeatedly with deionized water until the supernatant reached a pH above 6. The obtained solid was then treated with 1.5 g of LiCl dissolved in 25 mL of deionized water under vigorous shaking for 20 minutes. Following two additional washing steps (4500 rpm, 5 minutes each), the precipitate was redispersed in water. A dark colloidal dispersion formed, indicating the successful delamination of MXene. The few-layer Ti_3C_2 MXene nanosheets were isolated by centrifugation at 3500 rpm for 5 minutes, then filtered and freeze-dried under vacuum. Finally, the layered $\text{Ti}_3\text{C}_2\text{T}_x$ MXene powder was collected.

1.2 Synthesis of MIL-125(Ti)

A solvothermal method was used to synthesize MIL-125(Ti). First, 3 g of terephthalic acid was dissolved in 54 mL of *N,N*-dimethylformamide (DMF) under ultrasonic treatment. Separately, 1.56 mL of tetrabutyl titanate (TBOT, $\text{Ti}(\text{OC}_4\text{H}_9)_4$) was slowly introduced into 6 mL of methanol under vigorous stirring, resulting in a clear, colorless solution. This TBOT–methanol solution was then gradually added to the DMF–terephthalic acid solution while stirring continued for 30 minutes. During this process, the mixture transitioned from a light-yellow transparent liquid to a milky-white

suspension, indicating the initial formation of the framework. The homogeneous mixture was transferred into a 100 mL Teflon-lined autoclave and subjected to solvothermal treatment at 120 °C for 24 hours. After cooling to room temperature, the resulting precipitate was collected via centrifugation at 6000 rpm. DMF was used to rinse off residual unreacted ligands. Subsequently, the collected solids were further washed three times with 25 mL methanol to exchange the DMF solvents. At last, the solid was heated at 80°C in the vacuum oven.

1.3 Preparation of MIL-125(Ti)/MXene (MM)

Ti₃C₂ MXene@TiO₂/MIL-125(Ti) composite was synthesized by simple wet impregnation method. The synthesis method was as follows: 50 mg MIL-125(Ti) was added to methanol by ultrasonic for 1 hour, and then 20 mg Ti₃C₂ MXene was added to methanol and treated under ultrasonic for 2 hours. The MOF suspension was then transferred to the MXene solution for 4 hours. Then, the mixture was centrifuged (6500 rpm, 5 minutes) and vacuum-frozen for 48 hours. Finally, after grinding the dried product, MIL-125(Ti)/MXene (MM) was obtained.

1.4 Preparation of TiO₂@MIL-125(Ti)/MXene (MM-T)

65 mg MM was placed in a porcelain boat and sent into a muffle furnace for calcination in the air at 200, 300, 350, and 400 ° C respectively (the heating rate was set at 5°C /min). Under an air atmosphere, it was maintained at a constant temperature for 2 hours, until the sample cools naturally to room temperature. The final products are designated as MM-200, MM-300, MM-350 and MM-400.

2 Characterization

Powder X-ray diffraction (PXRD) patterns were collected on Bruker D8 advance with Cu K α radiation ($\lambda=1.5418 \text{ \AA}$). Scanning electron microscopy (SEM) images were obtained by Zeiss-Supra 55 at an acceleration voltage of 5 kV. Transmission electron microscopy (TEM) was recorded using JEM-2100, and energy dispersive spectrometer (EDS) elemental mapping images was captured on Tecnai G2 F30 S-TWIN at an acceleration voltage of 300 kV. FT-IR measurements are performed using Cary 610/670 (Varian Co.). Raman spectra were obtained via INVIA REFLEX (Renishaw),

in the range of 150-4000 cm^{-1} . The N_2 adsorption-desorption isothermals were obtained by Autosorb-Iq via Brunauer-Emmet-Teller (BET) method. The pore size was obtained from the adsorption-desorption branch of the nitrogen isotherms by the Barrett-Joyner-Halenda method. Thermogravimetry analysis (TGA) was performed under O_2 atmosphere from room temperature to 900 $^\circ\text{C}$ at a heating rate of 10 $^\circ\text{C min}^{-1}$.

X-ray photoelectron spectra (XPS) were collected with a Thermo Scientific ESCALAB 250Xi X-ray photoelectron spectrometer. All binding energies were calibrated using C 1s at 284.8 eV as a reference. The UV-vis diffuse reflectance spectra (UV-vis DRS) were obtained for the dry-pressed disk samples using a Cary 500 Scan UV-vis spectrophotometer (Varian). BaSO_4 was used as a reflectance standard in the UV-visible diffuse reflectance experiment. Photoluminescence (PL) was measured by an F-7000FL spectrometer.

In-situ Fourier transform infrared spectroscopy (FTIR) was performed by adopting a INVENIO S from Bruker, Germany, with a MCT detector. The sample (10 mg) was prepared as ink and dropped onto the ZnSe Crystal in the *in-situ* cell. After loading the sample, the background baseline was collected at room temperature. Pure N_2 was used to bubble water until saturation. Then, a 300W Xenon lamp (Beijing China Education Golden Light Co., LTD.) was turned on, and the spectrum was collected every 5 minutes for 60 minutes.

3 Photocatalytic N_2 fixation performance test

The experiments were carried out under ambient temperature and pressure using a 100 mL quartz reactor. A 300 W Xenon lamp (CEL-HXF300-T3, Beijing China Education Golden Light Co., Ltd.) equipped with a UVIRCut400 filter (400–780 nm) served as the visible light source. For each test, 25 mg of the photocatalyst was ultrasonically dispersed in 50 mL of deionized water. The suspension was then transferred into the quartz reactor and purged with N_2 gas under dark conditions for 30 minutes (400 rpm) to eliminate dissolved oxygen.

Subsequently, the reactor was irradiated with visible light ($\lambda = 400\text{--}780\text{ nm}$) from the Xenon lamp. Throughout the reaction, cooling water circulation was applied to maintain the temperature of the suspension at 25 $^\circ\text{C}$. Aliquots of 5 mL were withdrawn

at 30-minute intervals, and the catalyst was removed by filtration to obtain clear supernatant solutions. The concentration of ammonia in the samples was quantified using the Nessler's reagent method.

For cycling stability tests, 50 mg of photocatalyst was adopted and the other procedure was repeated. After each run, the used photocatalyst was recovered, washed with deionized water, and re-dispersed for the next cycle. The finally catalyst was washed with methanol and freeze-dried for further analysis.

4 Electrochemical measurements.

Electrochemical impedance spectra (EIS), photocurrent, and Mott-Schottky (MS) plots were performed on an electrochemical workstation (CHI660B, Shanghai Chenhua Co., China) with a three-electrode system. 0.1 M Na₂SO₄ aqueous solution was used as an electrolyte. EIS was carried out by applying a 50 mV alternating signal with a frequency of 100 kHz -0.01 Hz. The working electrode was prepared as follows: 5 mg catalyst was added in 700 μ L ethanol and 250 μ L deionized water, then sonicated for 15 min. Then, 50 μ L of Nafion was added and sonicated for another 15 minutes. After thorough homogeneous mixing, and 10 μ L was drop-casted onto ITO (1 \times 1 cm²). The as-prepared sample modified ITO, Pt wire, and Ag/AgCl electrode, which serve as a working electrode, counter electrode, and reference electrode, respectively.

5 Calculations

DFT, as implemented in Vienna ab initio simulation package (VASP), was used to carry out the calculations presented here. The projector augmented wave (PAW) method was used to treat the effective interaction of the core electrons and nucleus with the valence electrons, while exchange and correlation were described using the Perdew–Burke–Ernzerhof (PBE) functional. The cut-off energy is set at 600 eV for the plane-wave basis restriction in all calculations. K-points are sampled under the Monkhorst–Pack scheme for the Brillouin-zone integration (K-points were sampled using the Gamma Point). In all calculations, the forces acting on all atoms are < 0.02 eV/Å in fully relaxed structures, and self-consistency accuracy of 10⁻⁵ eV is reached for electronic loops.

The adsorption energy change (ΔE_{abs}) was determined as follows:

$$\Delta E_{\text{abs}} = E_{\text{total}} - E_{\text{slab}} - E_{\text{mol}}$$

where E_{total} is the total energy for the adsorption state, E_{slab} is the energy of pure surface, E_{mol} is the energy of adsorption molecule.

The free energy change (ΔG) for adsorptions were determined as follows:

$$\Delta G = E_{\text{total}} - E_{\text{slab}} - E_{\text{mol}} + \Delta E_{\text{ZPE}} - T\Delta S$$

where E_{total} is the total energy for the adsorption state, E_{slab} is the energy of pure surface, E_{mol} is the energy of adsorption molecule, ΔE_{ZPE} is the zero-point energy change and ΔS is the entropy change.

The calculated adsorption energy was obtained by the following equation:

$$\Delta E = E_{\text{AB}} - E_{\text{A}} - E_{\text{B}}$$

where E_{AB} represents the energy of the composites, and E_{A} and E_{B} represent the binding energy of the separated A and B, respectively.

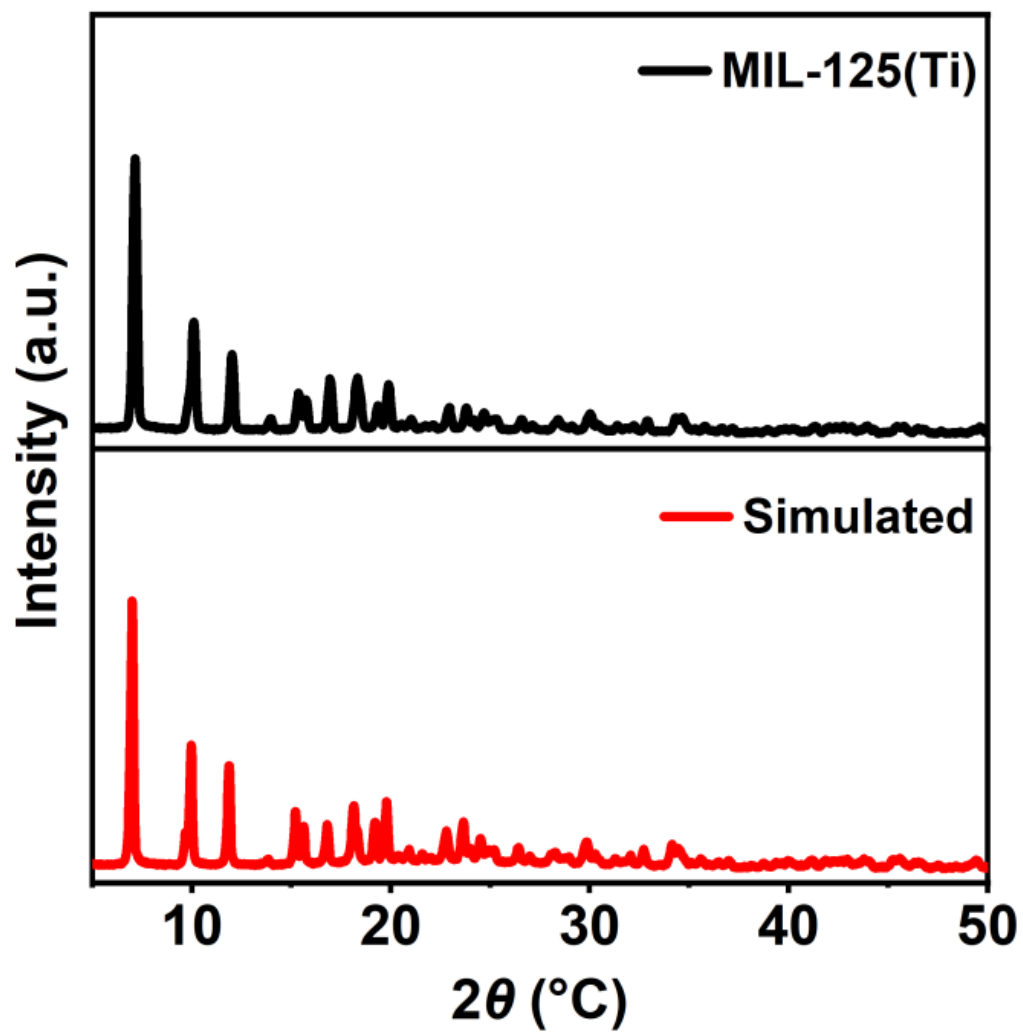


Figure S1. The XRD pattern of the simulated and synthesized MIL-125(Ti).

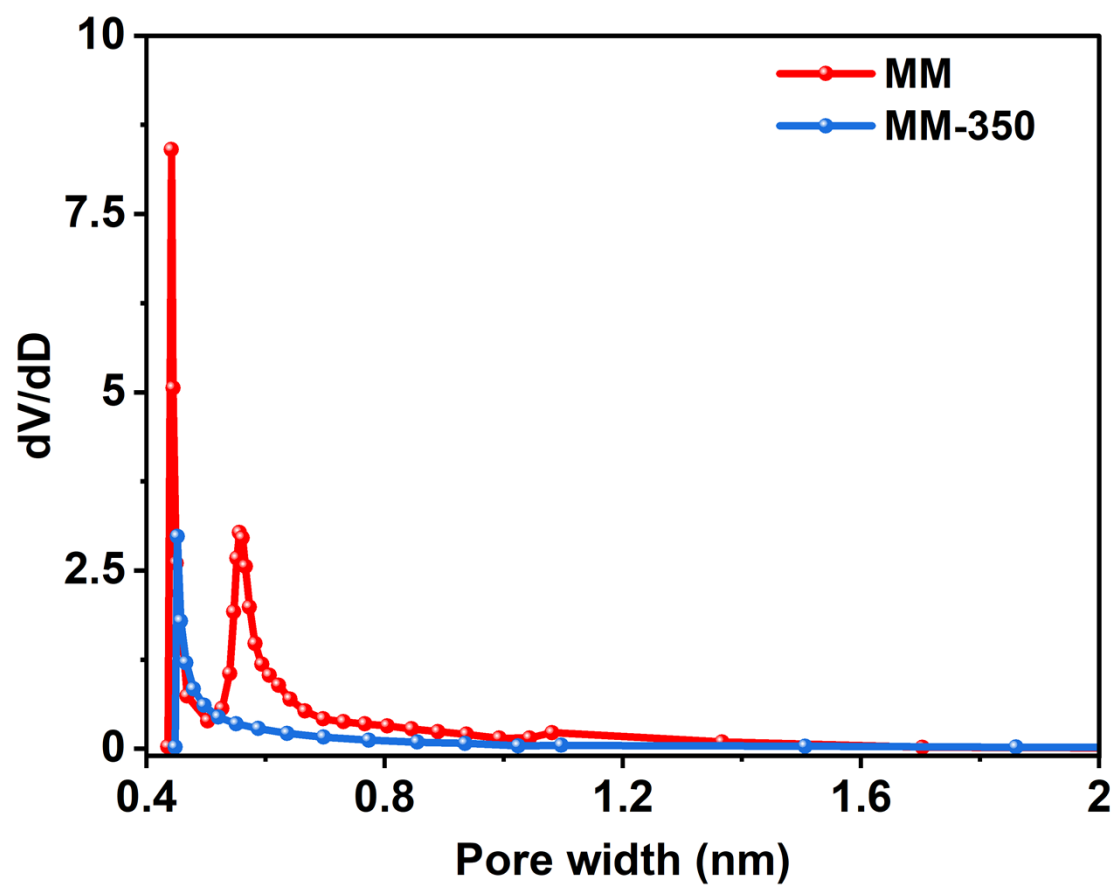


Figure S2. The pore size distribution of MIL-125(Ti) and MM-350.

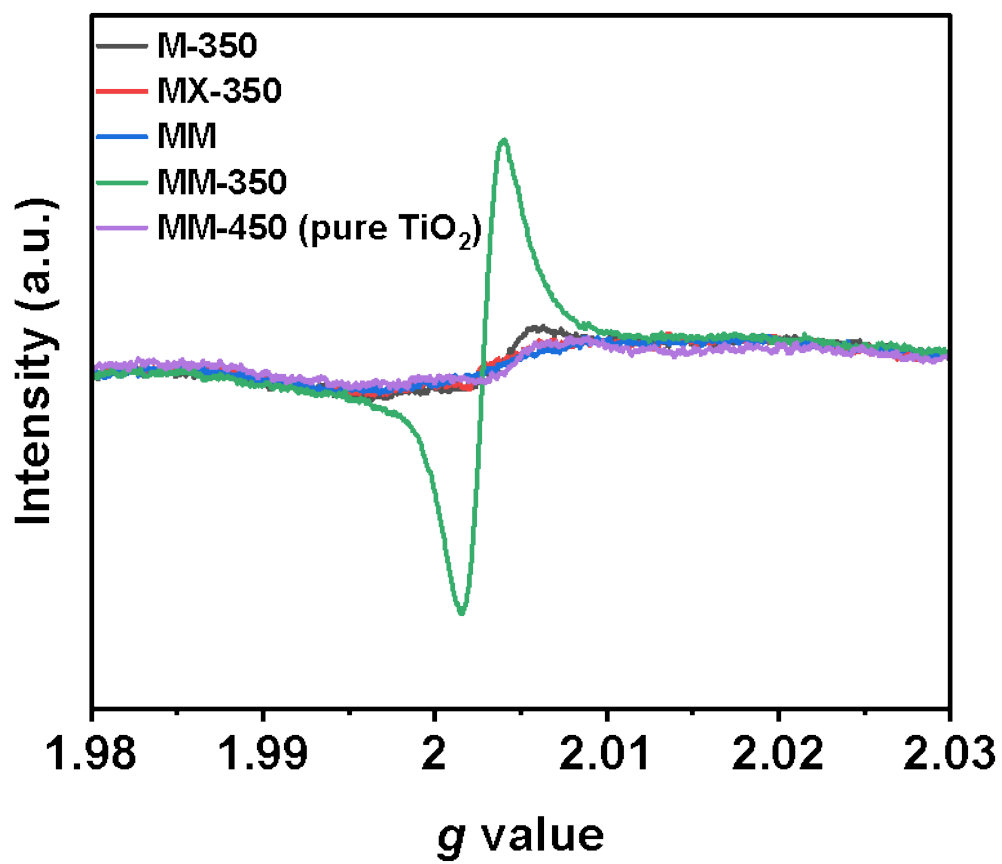


Figure S3. EPR spectra of M-350, MX-350, and MM-T.

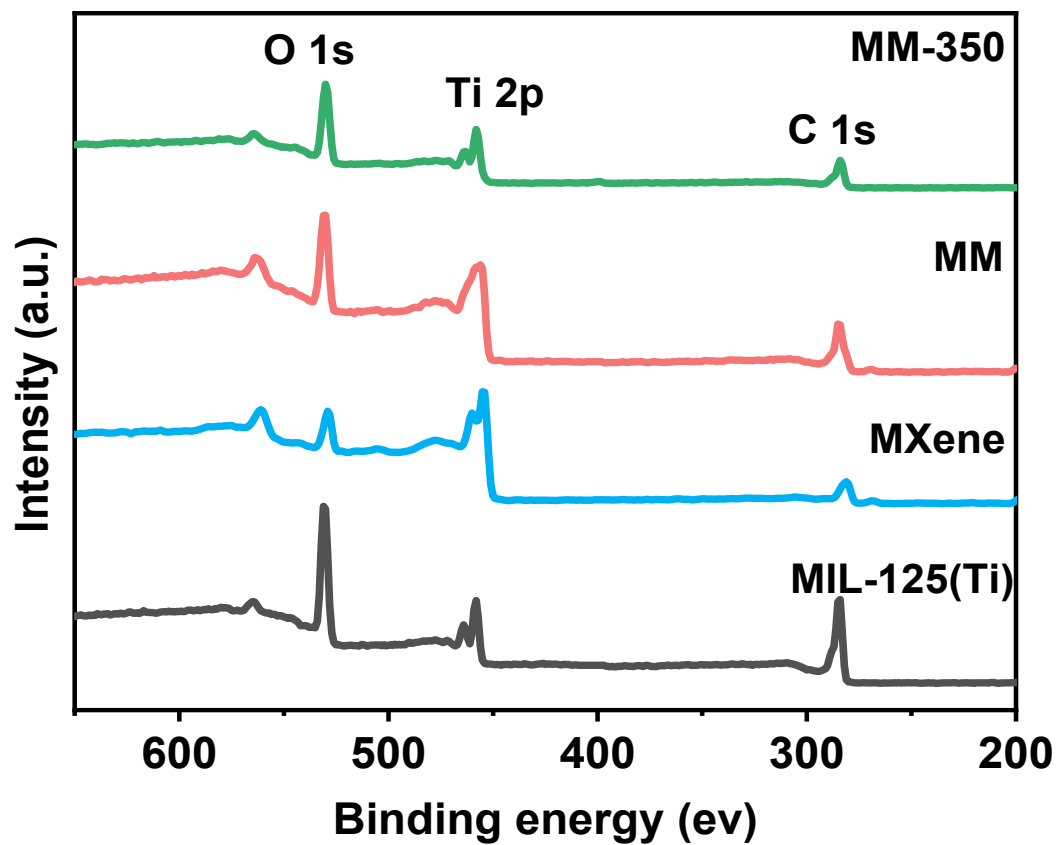


Figure S4. XPS survey spectra of MIL-125(Ti), MXene, MM, and MM-350.

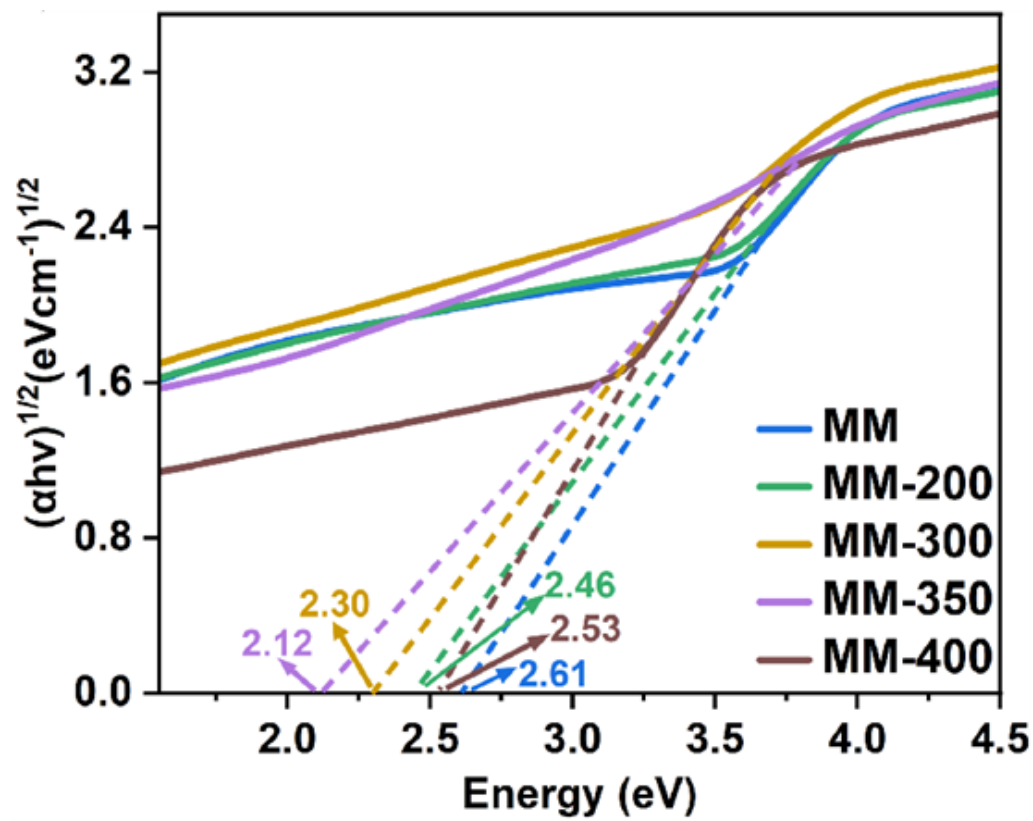


Figure S5. The plots of $(\alpha h\nu)^2$ versus $h\nu$.

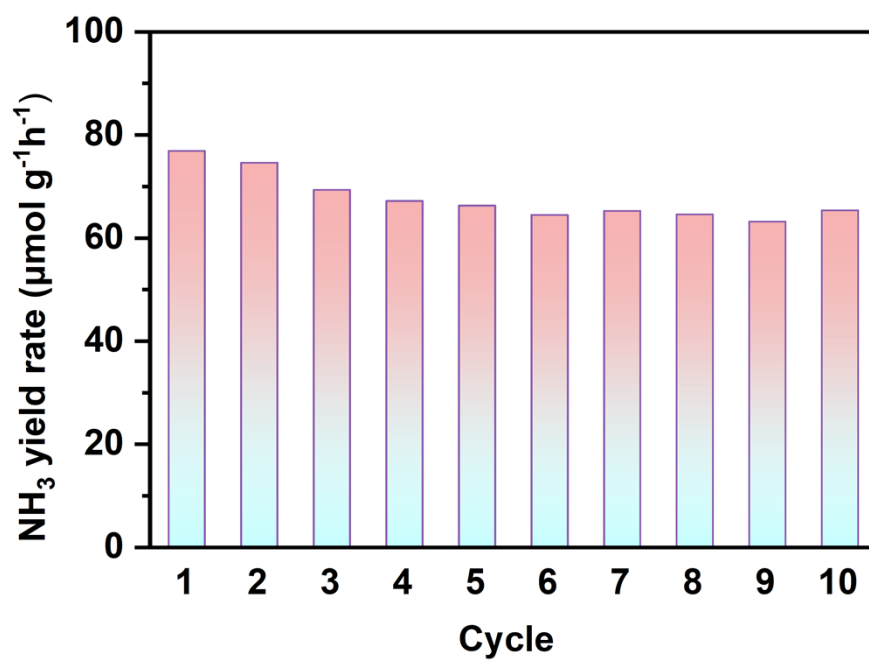


Figure S6. The long-term cycling stability experiment of MM-350.

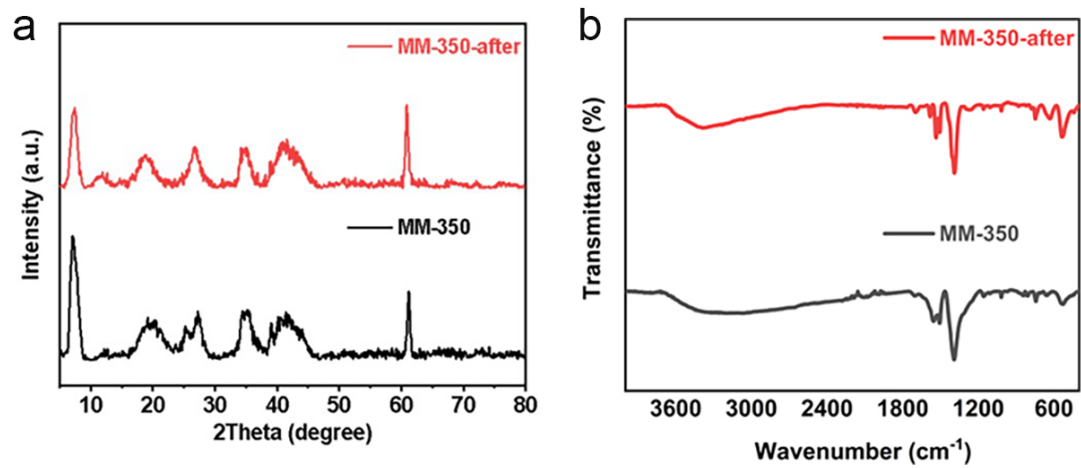


Figure S7. (a) XRD patterns, (b) IR spectra of MM-350 after the cycling tests.

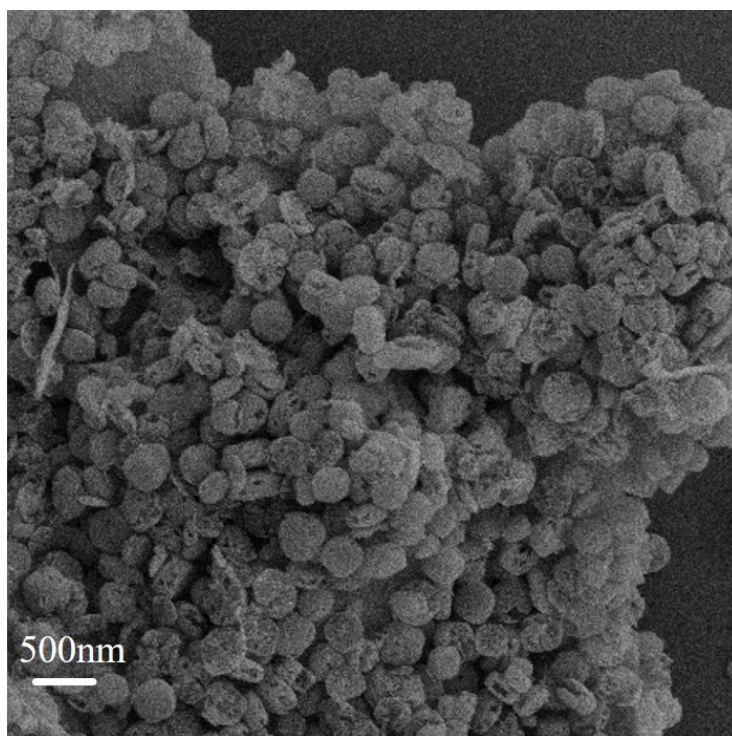


Figure S8. The morphology of MM after multi-cycle photocatalysis.

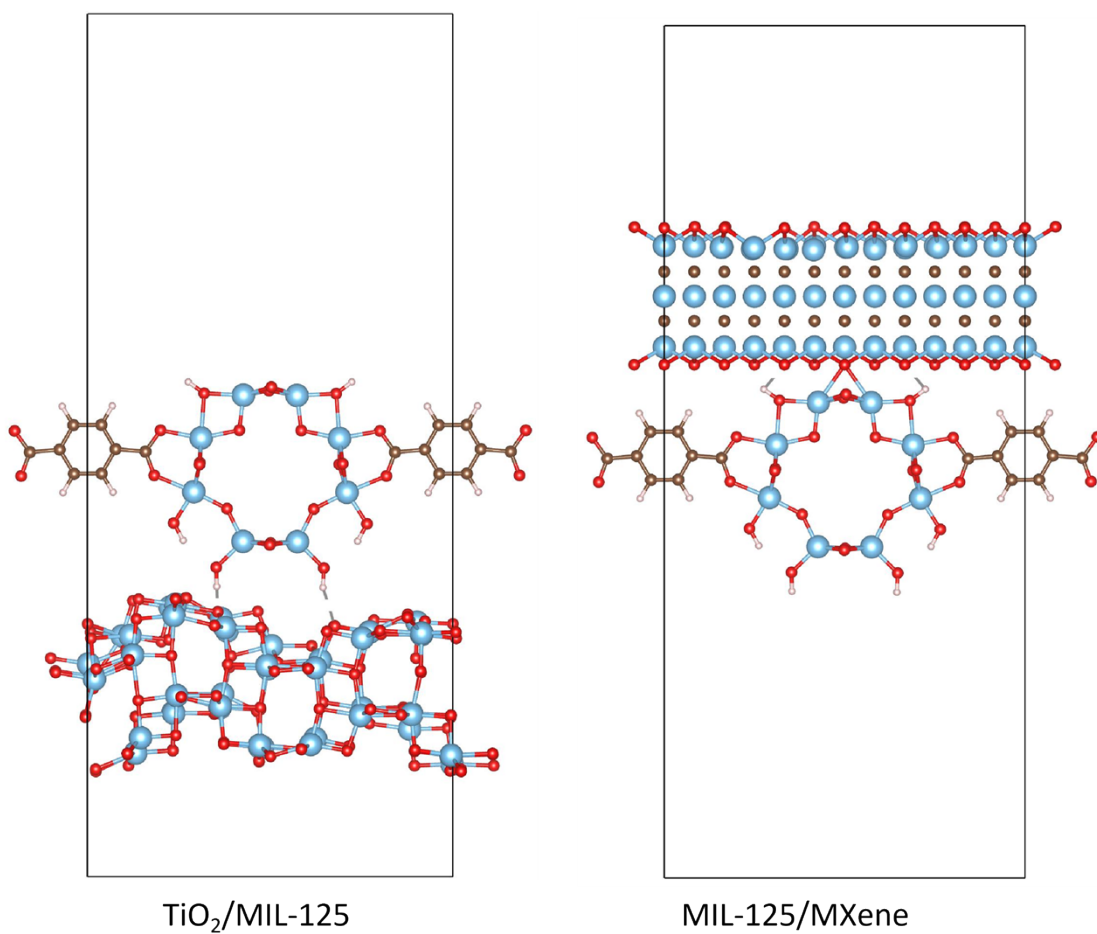


Figure S9. The model of the interface of $\text{TiO}_2/\text{MIL-125}$ and MIL-125/MXene.

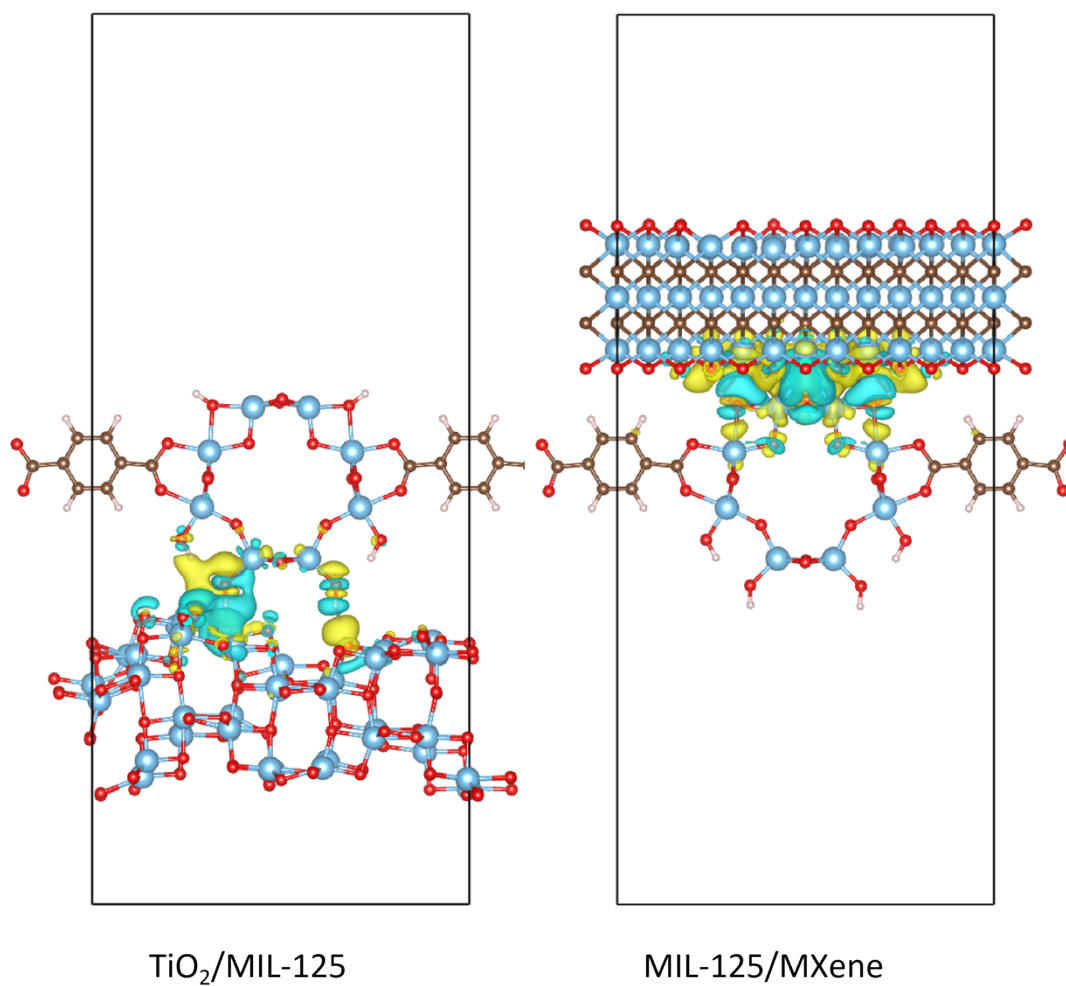


Figure S10. The charge density difference of TiO₂/MIL-125 and MIL-125/MXene.

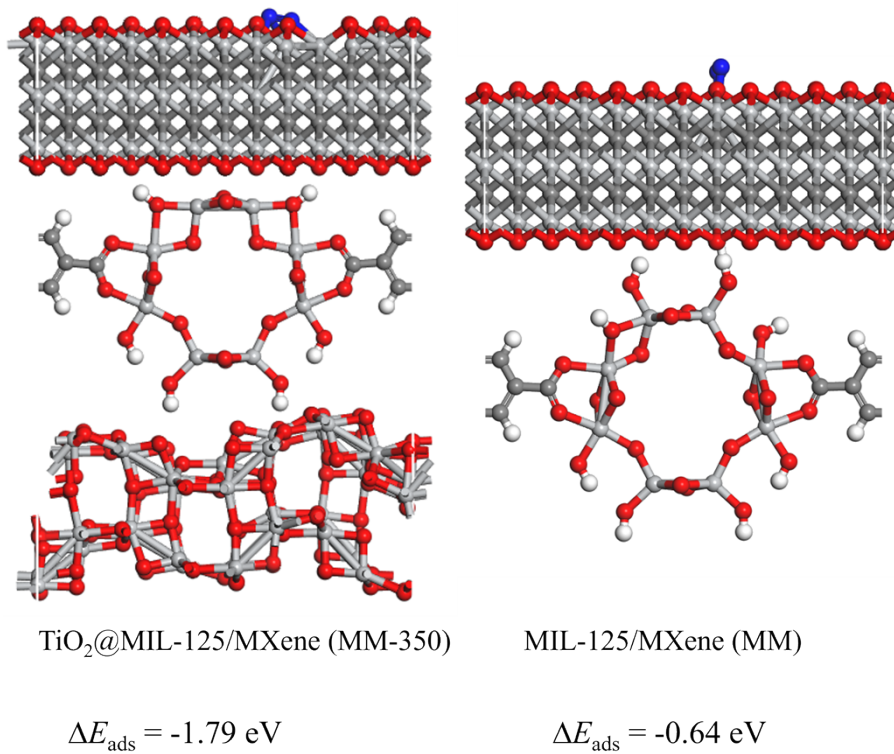


Figure S11. The N₂ adsorption energy of the optimized MM-350 and MM.

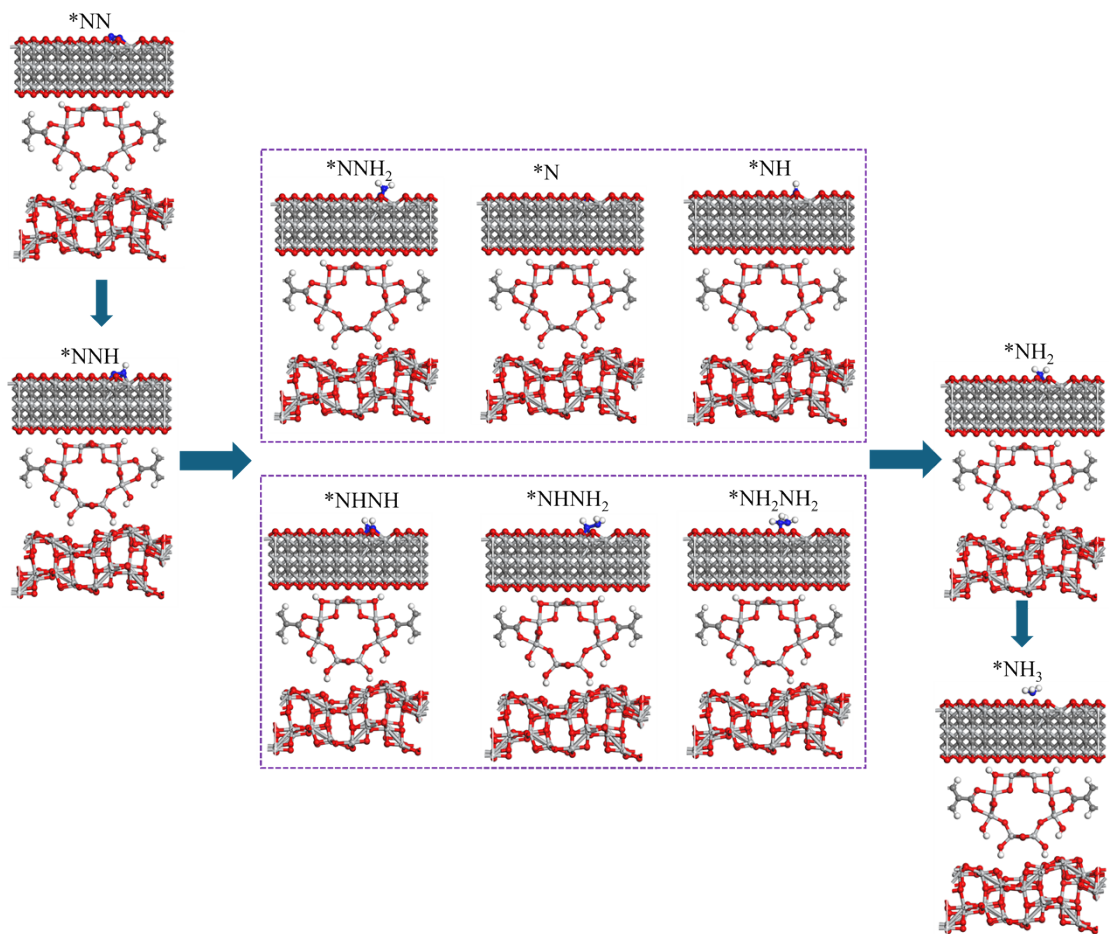


Figure S12. The theoretical models of the intermediates for MM-350 (up: distal pathway, down: alternating pathway).

Table S1. Representative MOF-based composites for photocatalytic N₂ fixation.

Catalyst	Light source	Sacrificial agents	active site	Measurement methods	Ammonia production rate	Refs
MM-350	Xenon Lamp (300W) $\lambda \geq 400$ nm	None	Zr sites	Nessler's reagent	76.92 $\mu\text{molg}^{-1}\text{h}^{-1}$	This work
Au@UiO-66	Xenon Lamp (300W) $\lambda \geq 400$ nm	None	Au sites	Nessler's reagent; Indophenol-blue	18.9 $\mu\text{molg}^{-1}\text{h}^{-1}$	[1]
ZIF-67@PMo ₄ V ₈	Xenon Lamp (300W) Full spectrum	None	POMs sites	Nessler's reagent	149 $\mu\text{molg}^{-1}\text{h}^{-1}$	[2]
MOF-74@C ₃ N ₄	Xenon Lamp (300 W)	K ₂ SO ₃	Zn sites	Nessler's reagent	330 $\mu\text{molg}^{-1}\text{h}^{-1}$	[3]
KNbO ₃ @TMU-5	UV irradiation (0.2 W)	ethanol	Ni sites	the indophenol method	39.9 $\mu\text{molL}^{-1}\text{h}^{-1}\text{g}^{-1}$	[4]
Ti ₃ C ₂ -QD/Ni-MOF	Xenon Lamp (300 W)	ethanol	Ti sites	Nessler's reagent	88.79 $\mu\text{molg}^{-1}\text{h}^{-1}$	[5]
Graphene-Ce-UiO-66	LED (3.5m W cm ⁻²)	None	C from Benzene	ammonia sensing electrode	50 $\mu\text{molg}^{-1}\text{h}^{-1}$	[6]
Bi ₄ O ₃ Br ₂ /ZIF-8	Xenon Lamp (300 W)	None	Bi	indophenol blue method	327.338 $\mu\text{molL}^{-1}\text{h}^{-1}\text{g}^{-1}$	[7]
MIL-125@TiO ₂	Xenon Lamp (300 W, 200	None	linker defects	indophenol blue method	102.7 $\mu\text{molg}^{-1}\text{h}^{-1}$	[8]

References

- 1 Chen L-W, Hao Y-C, Guo Y *et al.* Metal–Organic Framework Membranes Encapsulating Gold Nanoparticles for Direct Plasmonic Photocatalytic Nitrogen Fixation. *J Am Chem Soc*, 2021, **143**: 5727–5736.
- 2 Li X, He P, Wang T *et al.* Keggin-Type Polyoxometalate-Based ZIF-67 for Enhanced Photocatalytic Nitrogen Fixation. *ChemSusChem*, 2020, **13**: 2769–2778.
- 3 Ding Z, Wang S, Chang X, Wang D-H, Zhang T. Nano-MOF@defected film C₃ N₄ Z-scheme composite for visible-light photocatalytic nitrogen fixation. *RSC Adv*, 2020, **10**: 26246–26255.
- 4 Chamack M, Ifires M, Akbar Razavi SA *et al.* Photocatalytic Performance of Perovskite and Metal–Organic Framework Hybrid Material for the Reduction of N₂ to Ammonia. *Inorg Chem*, 2022, **61**: 1735–1744.
- 5 Qin J, Liu B, Lam K-H *et al.* 0D/2D MXene Quantum Dot/Ni-MOF Ultrathin Nanosheets for Enhanced N₂ Photoreduction. *ACS Sustain Chem Eng*, 2020, **8**: 17791–17799.
- 6 Liu S, Teng Z, Liu H *et al.* A Ce-UiO-66 Metal–Organic Framework-Based Graphene-Embedded Photocatalyst with Controllable Activation for Solar Ammonia Fertilizer Production. *Angew Chem Int Ed*, 2022, **134**: e202207026.
- 7 Liu J, Li R, Zu X *et al.* Photocatalytic conversion of nitrogen to ammonia with water on triphase interfaces of hydrophilic-hydrophobic composite Bi₄O₅Br₂/ZIF-8. *Chem Eng J*, 2019, **371**: 796–803.
- 8 Wang L, Wang S, Li M *et al.* Constructing oxygen vacancies and linker defects in MIL-125 @TiO₂ for efficient photocatalytic nitrogen fixation. *J Alloys Compd*, 2022, **909**: 164751.
- 9 Mansingh S, Subudhi S, Sultana S, Swain G, Parida K. Cerium-Based Metal–Organic Framework Nanorods Nucleated on CeO₂ Nanosheets for Photocatalytic N₂ Fixation and Water Oxidation. *ACS Appl Nano Mater*, 2021, **4**: 9635–9652.
- 10 Shen Z, Li F, Guo L *et al.* Ligand bridged MXene/metal organic frameworks heterojunction for efficient photocatalytic ammonia synthesis. *Appl Catal B Environ Energy*, 2024, **346**: 123732.

- 11 Ren H, Tan J, Zhao Z *et al.* Multi-stepwise electron transfer *via* MOF-based nanocomposites for photocatalytic ammonia synthesis. *Catal Sci Technol*, 2022, **12**: 5540–5548.